1-10-2018

Comparison of Inter and Intra-Operator Differences for Cephalometric Landmark Identification on Three-Dimensional CBCT Images using Pro Plan CMF

Timothy P. Levine
Jacobi Medical Center

Gregory J. Matthews
Loyola University Chicago, gmatthews1@luc.edu

Hugo F. Calero
Jacobi Medical Center

Victor M. Badner
Jacobi Medical Center

Recommended Citation

Levine TP, Matthews GJ, Calero HF, Badner VM. Comparison of Inter and IntraOperator Differences for Cephalometric Landmark Identification on Three-Dimensional CBCT Images using Pro Plan CMF. J Dents Dent Med. 2018 Jan;1(1):104

Boffin Access

Open Access Journal | Volume: 1.1

Journal of Dentistry and Dental Medicine

ISSN 2517-7389

Comparison of Inter and Intra-Operator Differences for Cephalometric Landmark Identification on Three-Dimensional CBCT Images using Pro Plan CMF

Timothy P. Levine[1]*
Gregory J. Matthews[2]
Hugo F. Calero[3]
Victor M. Badner[4]

[1]Director of Orthodontics, Department of Dentistry and OMFS, Jacobi Medical Center, Bronx, NY, USA
[2]Assistant Professor of Statistics, Loyola University Chicago, IL, USA
[3]Fellow, Surgical Orthodontics and Craniofacial Orthopedics, Jacobi Medical Center, Bronx, NY, USA
[4]Chair, Department of Dentistry and OMFS, Jacobi Medical Center, Bronx, NY, USA

Abstract

Objective: To establish reliability of cephalometric landmark identification in three-dimensions using ProPlan CMF software.

Methods: Two orthodontist identified a series of 33 cephalometric landmarks on 20 CBCT scans of Class I, pre-orthodontic patients and repeated the landmark identification about two months later. Intraclass correlations (ICC) were calculated by landmark in the X, Y, and Z dimensions and F-test were used to assess difference in landmark location in the X, Y, and Z dimensions.

Results: The majority of landmarks had good to excellent ICC for both inter- and intra-observer reliability. F-test also showed the majority of landmarks had no significant difference between the observers.

Conclusion: Most landmarks showed good to very good reliability and reproducibility using ProPlan CMF, with some landmarks proving more reliable than others and further research is needed to establish the utility and practicality of three-dimensional cephalometrics as a common diagnostic tool in orthodontics

Keywords

Dentistry; Orthodontics; Oral surgery; Three-Dimension imaging

Introduction

Broadbent introduced cephalometric analysis in 1931[1]. The tool quickly became a critical element in the study and diagnosis of malocclusion and skeletal issues that contribute to malocclusion. Through comparison with established normal values, linear and angular measurements on lateral cephalograms can be used to define relational issues with the teeth and the skeletal structure of the face.

There are numerous limitations to two-dimensional cephalometrics [2]. For one, an entire dimension of measurement is lost by necessity when a three-dimensional object is projected on a two-dimensional film. This also creates artifacts from overlapping structures and magnification of areas of the subject that are farther from the film. Repeating cephalometric films is difficult in practice and even small subject positioning changes can artificially alter relationships between points of interest. Studies show that two-dimensional projections inadequately reflect clinical diagnoses [2,3].

Three-dimensional radiography with cone beam computed tomography (CBCT) can allow clinicians to improve accuracy of diagnosis and treatment planning [4]. The image is three-dimensional, eliminating the projection errors and making irrelevant distortion and magnification issues inherent in two-dimensional imaging. Its main drawback, increased radiation compared to traditional panoramic or lateral cephalometric films, is mitigated by the fact that the sum of radiation exposure of a standard orthodontic patient, including a lateral and posterior-anterior cephalograms, panoramic and periapical films, is similar to or even more than a single CBCT [5]. Orthodontists have to adjust to using CBCTs, should they become standard, as most practicing orthodontists were only trained in two-dimensional cephalometrics. Additionally, studies must be done to validate cephalometric analysis of CBCTs and to establish reliability and reproducibility between operators. An additional consideration must be made for software, as well, as CBCTs are a purely digital medium and different software packages present different viewing and tracing options. A number of studies have examined the accuracy of CBCTs converted to two-dimensional films and the reproducibility of landmark identification, the reliability of linear measurements, and reliability of landmark identification between multiple operators [6-14]. No current study has established reliability and reproducibility using ProPlan CMF (Materialise, Belgium),

Article Information

DOI: 10.31021/jddm.20181104
Article Type: Research Article
Journal Type: Open Access
Volume: 1 **Issue:** 1
Manuscript ID: JDDM-1-104
Publisher: Boffin Access Limited

Received Date: December 12, 2017
Accepted Date: December 28, 2017
Published Date: January 10, 2018

*Corresponding author:

Levine TP, DMD
Director of Orthodontics
Dept of Dentistry
Jacobi Medical Center, Bronx, NY, USA
Consultant in Orthodontics in Dental Planet
Tel no: 718-918-5635
E-mail: timothy.levine@nychhc.org

Citation: Levine TP, Matthews GJ, Calero HF, Badner VM. Comparison of Inter and IntraOperator Differences for Cephalometric Landmark Identification on Three-Dimensional CBCT Images using Pro Plan CMF. J Dents Dent Med. 2018 Jan;1(1):104

a common software package used in planning orthognathic surgery.

The aims of this study were to assess intra- and inter-operator observer reliability in located anatomic landmarks on the hard tissue of the skull using ProPlan CMF on images produced via CBCT.

Subject and Methods

Institutional review board approval was obtained. Twenty (N=20) pre-treatment CBCTs were collected from a private orthodontic office whose routine pre-treatment records include CBCT images. Images were obtained on an Orthophos XG 3D (Sirona Dental Systems, New York City) operated via a personal computer running Windows 7 operating system (Microsoft Corporation, Redmond, WA). Records were anonymized, removing all identifying information, and given a unique identifier. Ten female and 10 male patients (average age 14.7 years, range 11.0 to 20.1 years) were selected. Each scan was assessed to assured all points were viewable on the image, with a field of 8 cm^3 and resolution of 160 µm. The raw image was processed by Sidexis NG (Sirona) and exported into a DICOM (Digital Imaging and Communications in Medicine) file. The file was then imported into ProPlan CMF on a dedicated laptop running Windows 7 (Figure 1). A volumetric model was generated via ProPlan CMF.

Two orthodontists, were trained and calibrated on the ProPlan CMF software, with assistance from Materialise customer support. Each observer was given several weeks and five "practice" scans not included in this study in order to become acquainted with and calibrated to the software. Following the calibration period, the operators identified 33 points cephalometric points, commonly used in the Downs, Steiner and Grummons analyses, listed in Table 1, with definitions of locations adapted from de Oliveira [15,16]. All points were identified on each CBCT (T1). Sixty to 80 days later (T2), the 20 CBCTs were re-ordered, and the operators repeated the identification. The ProPlan CMF software then produced numerical values for the X (coronal plane), Y (axial plane), and Z (sagittal plane) coordinates for each point, exported into a comma-separated values (CSV) file, yielding 40 sets of 99 observations for each observer.

For each of the landmarks in each dimension, intra-observer reliability and inter-observer reliability were estimated using intraclass correlation (ICC), with ICC at or above .9 evaluated as "excellent reliability", .9 to .75 as "good reliability", .75 to .45 as "fair reliability" and below .45 as "weak reliability" [17].

An F-test was calculated for the X, Y and Z coordinates of each landmark to test the null hypothesis that there was no significant difference in the mean location of landmarks by each observer. The Family Wise Error Rate (FWER) was set at alpha = .05 and the Hochberg correction for multiple hypothesis testing were used to control the FWER [18]. The sample size of this study was chosen based on sample sizes from similar studies [19]. Therefore, rather than performing a sample size calculation, effect size was calculated based on the sample. This power calculation was performed using a simulation study with 500 simulations per effect size. For the simulation, we assumed that the error variance was 0.5 and the variance component associated with the patient was 2.2 where these values were calculated from the observed data. In each replicate of the simulation, data was generated assuming different effect sizes and an F-test was performed testing the null hypothesis that the mean difference between the doctors was 0 versus the alternative that the mean difference was non-zero.

Results

Power was calculated using 500 simulations per effect size, with error variance set to 0.5 and variance component set to 2.2, with these values calculated from observed data. In each replicate of the simulation, data was generated using different effect sizes. An F-test was performed on the null hypothesis, producing 80 per cent power at an effect size just above 0.3. As the coordinates were a whole number system, an effect size of 0.3 was deemed very satisfactory.

ICC estimated reliability for each coordinate for each landmark: Table 2 displays all ICC results, by landmark, for both intra- and inter-observer reliability. Table 3 summarizes the ICC estimates for intra-observer reliability and Table 4 summarizes the ICC estimates for inter-observer reliability. Overall, the tables show that ICC

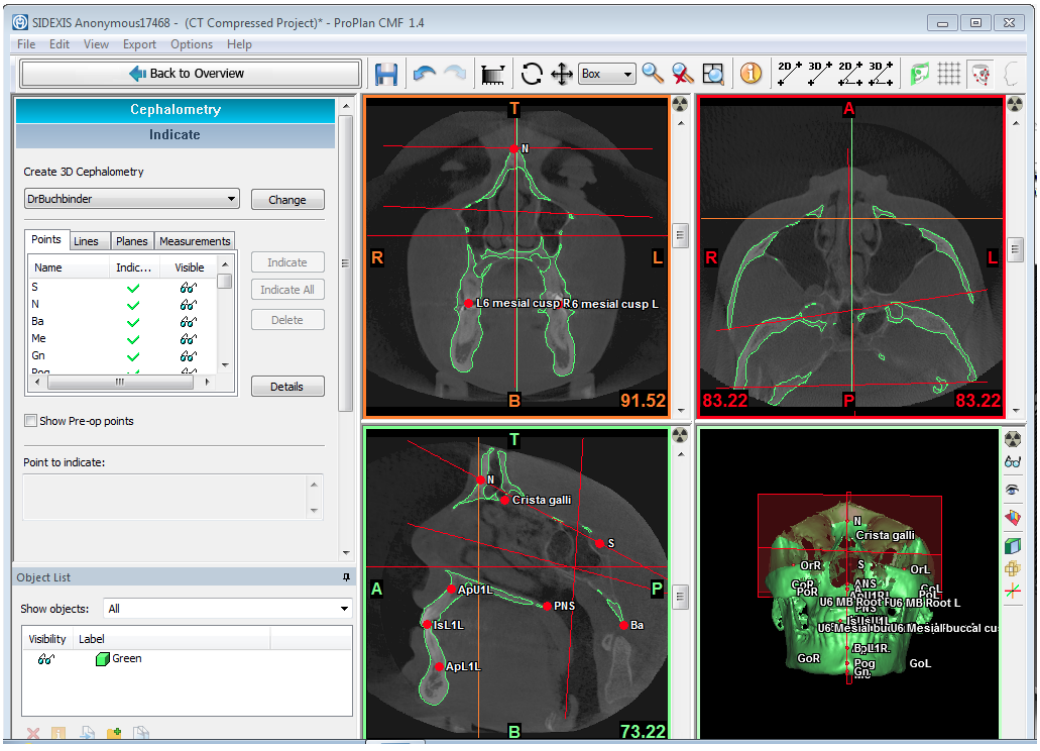

Figure 1: A screenshot of ProPlan CMF, demonstrating the multi-planar views and 3D model of a CBCT scan, including the landmarks identified. Reproduced with permission from Materialise.

Landmark	Anatomic Region	Coronal	Axial	Sagittal
A	Premaxilla	Posterior-most point on the curve of the maxilla between the anterior nasal spine and supradentale	Midpoint of anteroposterior and lateral width of fossa	Midpoint of lateral width of fossa
ANS	Median, sharp bony process of the anterior maxilla	Point on the tip	Anterior-most point	Midpoint of lateral width
ApL1L	Apex of root of lower left central incisor	Inferior-most point	Most inferior point along root axis	Point of the tip
ApL1R	Apex of root of lower right central incisor	Inferior-most point	Most inferior point along root axis	Point of the tip
ApU1L	Apex of root of upper left central incisor	Superior-most point	Most superior point along root axis	Point of the tip
ApU1R	Apex of root of upper right central incisor	Superior-most point	Most superior point along root axis	Point of the tip
B	Anterior surface of the mandibular symphysis	Posterior-most point	Middle-anterior-most point on the anterior contour	Middle point
Ba	Anterior surface of foramen magnum	Most anterior point	Midpoint of anterior edge	Most anterior point
CoL	Left condyle	Superior-most point	Middle point in the axial slice level determined by the lateral and anteroposterior views	Middle Superior-most point
CoR	Right condyle	Superior-most point	Middle point in the axial slice level determined by the lateral and anteroposterior views	Middle Superior-most point
Crista galli	Median ridge of cribiform plate of ethmoid	Anterior-superior most point	Midpoint of anterior portion of lateral width	Anterior-superior most point
Gn	Contour of the bony chin	Anterior-inferior- most point	Middle-anterior-inferior- most point	Middle-inferior-most point
GoL	Angle of the left mandibular body	Middle point along the angle	Posterior-most point	Inferior-most point
GoR	Angle of the right mandibular body	Middle point along the angle	Posterior-most point	Inferior-most point
IsL1L	Incisal tip of left lower central incisor	Superior-most point	Middle point of the mesiodistal and buccolingual width	Middle point of the mesiodistal width
IsL1R	Incisal tip of right lower central incisor	Superior-most point	Middle point of the mesiodistal and buccolingual width	Middle point of the mesiodistal width
IsU1L	Incisal tip of left upper central incisor	Inferior-most point	Middle point of the mesiodistal and buccolingual width	Middle point of the mesiodistal width
IsU1R	Incisal tip of right upper central incisor	Inferior-most point	Middle point of the mesiodistal and buccolingual width	Middle point of the mesiodistal width
L6 mesial cusp L	Mesiobuccal cusp tip of lower left first molar	Superior-most point along mesial cusp	Superior-most point along mesial cusp	Superior-most point along mesial cusp
L6 mesial cusp R	Mesiobuccal cusp tip of lower right first molar	Superior-most point along mesial cusp	Superior-most point along mesial cusp	Superior-most point along mesial cusp
Me	Lower border or the mandible	Inferior-most point	Middle-inferior-most point	Inferior-most point
N	Frontonasal suture	Anterior-most point	Middle-anterior-most point on the anterior contour	Middle point
OrL	Latero-inferior contour of the left orbit	Anterior-superior- most point on the edge between the internal and external contours	Anterior-most point	Latero-inferior point most
OrR	Latero-inferior contour of the right orbit	Anterior-superior- most point on the edge between the internal and external contours	Anterior-most point	Latero-inferior point most
PNS	Median, sharp bony process of the posterior maxilla	Point on the tip	Posterior-most point	Midpoint of lateral width
Pog	Contour of the bony chin	Anterior-most point	Middle-anterior-most point on the anterior contour	Middle point
PoL	Margin of left external auditory meatus of temporal bone	Superior point of rim of external auditory meatus	Superior point of rim of external auditory meatus	Superior point of rim of external auditory meatus
PoR	Margin of right external auditory meatus of temporal bone	Superior point of rim of external auditory meatus	Superior point of rim of external auditory meatus	Superior point of rim of external auditory meatus
S	Pituitary fossa of the sphenoidal bone	Middle point of the anteroposterior width of the fossa	Middle point of the anteroposterior and lateral width of the fossa	Middle point of the lateral width of the fossa
U6 MB Root L	Apex of mesiobuccal root of upper left central first molar	Superior-most point	Most superior point along root axis	Point of the tip
U6 MB Root R	Apex of mesiobuccal root of upper right central first molar	Superior-most point	Most superior point along root axis	Point of the tip
U6 Mesial buccal cusp L	Mesiobuccal cusp tip of lower left first molar	Inferior-most point along mesial cusp	Inferior-most point along mesial cusp	Inferior-most point along mesial cusp
U6 Mesial buccal cusp R	Mesiobuccal cusp tip of lower left first molar	Inferior-most point along mesial cusp	Inferior-most point along mesial cusp	Inferior-most point along mesial cusp

Table 1: A list of 33 cephalometric points, commonly used in the Downs, Steiner and Grummons analyses, with corresponding anatomic locations in each dimension

indicated excellent reliability for bother intra- and inter-observer assessments. Table 5 shows the F-test results for all landmarks, which indicated general agreement between the observers.

In 78 (79.79%) of intra-observations, ICC estimates were > 0.9, and 97 (97.98%) were > 0.75. Only two landmarks (2.12%) were < 0.75 (Z coordinate of Apex LR1 and Y coordinate of menton), and none were < 0.45. Midline structures (A, B, N, ANS, PNS, Gn, Me, Pog, S, crista galli, Ba) had better overall reliability with 32 of 33 coordinates > 0.75; only menton's Y coordinate was under 0.75. Lateral structures (left and right of each Or, Co, Go, Po, incisal tip of upper and lower 1s, apices of upper and lower 1s, MB cusp of lower 6s, MB cusp of U6s, and apices of upper 6s) had 65 coordinates > 0.75; only the apex of LR1 was below.

Intra-observer reliability ICC had 73 landmarks (73.74%) with estimates > 0.90, and 94 (96.9%) were > 0.75. Five of the remaining landmarks were > 0.45 (X coordinates for Incisal of UR1, left and right Or, Y coordinate for menton, Z coordinate for apex LR1); none were below 0.45. Midline structures had 32 of 33 coordinates (97.0%) above 0.75, and lateral structures had 62 of 66 coordinates (93.9%) above 0.75.

Table 5 shows the results of the F-test, which had 87 of 99 (87.88%) of observations with no significant difference in coordinates. The results for the X coordinates indicated that only four of the 33 (12%- GoR, MB Cusp L6R, OrL, OrR) produced significant results. In the Y dimension, seven observations (21.2%- apices of all four central incisors, Ba, Incisal L1L, Or R) produced significant results. The Z coordinates showed all but one coordinate with a non-significant result (3.0%- apex L1L).

Discussion

Cephalometrics, as developed by Broadbent and Hofrath decades ago, uses linear and angular measurements based on landmarks on two-dimensional film [1]. CBCTs offer three-dimensional images of three-dimensional objects, e.g. the human skull, eliminating the translation into two-dimensions required by traditional cephalometry.

As pointed out by Zamora, two-dimensional cephalometrics

	Intra-observer			Inter-observer		
Landmark	X	Y	Z	X	Y	Z
A	0.912	0.982	0.959	0.904	0.982	0.959
ANS	0.920	0.980	0.956	0.897	0.981	0.950
B	0.914	0.970	0.930	0.842	0.969	0.916
Ba	0.946	0.985	0.991	0.946	0.982	0.991
Crista galli	0.907	0.980	0.900	0.907	0.980	0.900
Gn	0.869	0.905	0.876	0.866	0.905	0.873
Me	0.874	0.579	0.833	0.823	0.579	0.833
N	0.952	0.989	0.949	0.940	0.985	0.949
PNS	0.922	0.969	0.984	0.908	0.958	0.980
Pog	0.864	0.935	0.839	0.852	0.935	0.770
S	0.895	0.985	0.995	0.895	0.983	0.994
ApL1L	0.873	0.969	0.924	0.866	0.961	0.890
ApL1R	0.842	0.963	0.621	0.787	0.939	0.621
ApU1L	0.949	0.982	0.933	0.906	0.982	0.933
ApU1R	0.949	0.980	0.780	0.935	0.980	0.754
CoL	0.925	0.979	0.994	0.925	0.979	0.993
CoR	0.970	0.985	0.992	0.966	0.980	0.989
GoL	0.951	0.929	0.976	0.926	0.929	0.975
GoR	0.978	0.927	0.969	0.963	0.916	0.954
IsL1L	0.880	0.984	0.925	0.826	0.984	0.917
IsL1R	0.895	0.986	0.927	0.867	0.984	0.927
IsU1L	0.800	0.985	0.932	0.769	0.985	0.932
IsU1R	0.756	0.977	0.939	0.686	0.974	0.937
L6 mesial cusp L	0.947	0.969	0.969	0.938	0.969	0.967
L6 mesial cusp R	0.890	0.971	0.969	0.890	0.969	0.969
OrL	0.761	0.984	0.964	0.704	0.984	0.964
OrR	0.876	0.981	0.974	0.669	0.979	0.969
PoL	0.897	0.981	0.993	0.897	0.972	0.991
PoR	0.894	0.980	0.991	0.753	0.975	0.982
U6 MB Root L	0.920	0.984	0.971	0.917	0.984	0.961
U6 MB Root R	0.912	0.983	0.979	0.880	0.980	0.967
U6 Mesial buccal cusp L	0.915	0.970	0.968	0.890	0.970	0.963
U6 Mesial buccal cusp R	0.940	0.962	0.976	0.931	0.962	0.972

Table 2: Intraclass correlation coefficients for all landmarks for intra- and inter-observer reliability

Range	X		Y		Z		All dimensions	
	N	%	N	%	N	%	N	%
1 > ICC > .9	18	55%	32	97%	28	85%	78	79%
.9 > ICC > .75	15	45%	0	0%	4	12%	19	19%
.75 > ICC > .45	0	0%	1	3%	1	3%	2	2%
.45 >ICC	0	0%	0	0%	0	0%	0	0%

Table 3: Intraclass Correlation Coefficients for intra-observer reliability

Range	X		Y		Z		All dimensions	
	N	%	N	%	N	%	N	%
1 > ICC > .9	14	42%	32	97%	27	82%	73	74%
.9 > ICC > .75	16	48%	0	0%	5	15%	21	21%
.75 > ICC > .45	3	9%	1	3%	1	3%	5	5%
.45 > ICC	0	0%	0	0%	0	0%	0	0%

Table 4: Intrarclass Correlation Coefficients for inter-observer reliability

are images of a three-dimensional skull into two dimensions, rather than specific points on specific bones [19]. This fact hinders any study that attempts to directly apply traditional cephalometrics into CBCTs. Points such as sella, defined broadly as the geometric center of sella turcica, have a new variable, the third dimension, which creates greater variation in identification [19,20]. As per de Oliveira, in these situations there is a natural tendency to identify landmarks in one or two planes that are easily visualized and while disregarding a plane where the point is difficult to visualize [16].

This fact is emphasized in the present study by the weak reliability of the landmarks' X dimension coordinates, representing the coronal plane; the coronal plane is the plane that is not represented in traditional cephalometry. This was true for both intra- and inter-observer reliability. Even with this increased difficulty, the present study found that overall reliability was excellent. Additionally, ProPlan CMF allows the CBCTs to be viewed in multiplanar (i.e., sagittal, axial and coronal) views as well as volumetric reconstructions. Several studies have shown this to improve reliability of landmark identification [13,14,18,21].

Overall, the present study agrees with previous studies that landmark identification in CBCTs is reliable and reproducible. It also suggests that ProPlan CMF is a program in which three-dimensional cephalometrics can be performed with confidence. The estimates of reliability for both intra- and inter-observer reliability were satisfactory, as no measurement had a coefficient that would be rated "poor" by ICC and only seven out of 198 total observations falling between 0.75 and 0.45, the range rated as "fair." All other observations, (n=191 (96.46%) were rated as "good" and 151 is rated as "excellent." (0.9) Furthermore, the F-test found that 87 of 99 (87.99%) of the observations of the coordinates had no significant difference.

The general trend in the present study matched previous studies, in that midline structures show high reliability when translated into three-dimensional cephalometrics [13,14,18,22,23]. The 11 midline structures showed excellent reliability in all dimensions for both intra- and inter-observer reliability with the exception of menton, which rated as "good" in the X and Z dimensions and only "fair" in the Y dimension. The F-test produced a significant result from a single coordinate for a midline structure, the Y coordinate of basion. The lateral skeletal structures showed overall good to excellent reliability with the ICC. Left orbitale in the X plane for both inter- and intra-operator observations and right and right orbitale for inter-operator in the X plane were both under 0.75. The F-test also produced significant results for X coordinate for both left and right orbitales and the Y coordinate for the right orbitale. Right gonion in the X dimension was the only other lateral skeletal structure to produce a significant F-test result. De Oliveira suggested that discrepancies in landmarks identification are likely due to inadequate definitions of the points in space and not a clear definition as to where they are on curved surfaces, which is consistent with the limitations of translating cephalometric language for three dimensions images.

Dental structures fared somewhat worse than skeletal structures, with ICC estimates in both intra- and inter-operator reliability. Apex of lower right central in the X plane for both inter- and intra-operator observations and the incisal tip of upper right central for inter-operator observations were below 0.75 and only rated "fair." Seven of the 11 significant results of the F-test in the present study were for dental structures. Katkar et al. had previously found that dental points were less reliably identifiable on CBCTs while Zomora concluded that dental landmark location was more highly reproducible [14,24]. The present study agrees with Katkar's

Landmark	X	Y	Z
A	0.979	0.976	0.959
ANS	0.979	0.174	0.959
ApL1L	0.979	**0.001	**0.001
ApL1R	0.979	**0.001	0.152
ApU1L	0.979	**0.001	0.599
ApU1R	0.979	*0.003	0.959
B	0.979	0.976	0.089
Ba	0.979	0.006	0.959
CoL	0.979	0.976	0.959
CoR	0.698	0.649	0.959
Crista galli	0.979	0.112	0.959
Gn	0.979	0.976	0.665
GoL	0.979	0.976	0.089
GoR	*0.026	0.976	0.959
IsL1L	0.979	*0.023	0.959
IsL1R	0.979	0.570	0.959
IsU1L	0.979	0.976	0.959
IsU1R	0.979	0.976	0.959
L6 mesial cusp L	0.113	0.976	0.770
L6 mesial cusp R	*0.036	*0.050	0.505
Me	0.979	0.976	0.959
N	0.979	0.976	0.959
OrL	**0.001	0.976	0.959
OrR	**0.001	*0.007	0.959
PNS	0.979	0.976	0.959
Pog	0.979	0.976	0.426
PoL	0.979	0.976	0.959
PoR	0.387	0.976	0.959
S	0.863	0.976	0.959
U6 MB Root L	0.979	0.976	0.959
U6 MB Root R	0.979	0.976	0.829
U6 Mesial buccal cusp L	0.979	0.976	0.959
U6 Mesial buccal cusp R	0.636	0.976	0.150

Table 5: F-test (alpha = 0.05) results for all landmarks (* $p \leq 0.5$, ** $p < 0.01$)

findings that, at least with the 160 μm resolution of scans used here, dental landmarks are indeed less reliably identified.

The current study used ProPlan CMF, an extremely common software package for planning orthognathic surgeries. Based on the results of the F-test and ICC, ProPlan appears to be a reliable program for three-dimensional cephalometrics. Lisboa noted that there are a paucity of three-dimensional cephalometric analysis software, thus it is important to test the reliability of those available to us. Two-dimensional cephalometrics remains the standard in orthodontics; the cost, increased exposure and the time investment required for landmark identification in three dimensions all remain obstacles [5,18]. Three-dimensional cephalometrics has to overcome these barriers before it can displace two-dimensional evaluation as the standard diagnostic tool.

References

1. Broadbent H. A new x-ray technique and its application to orthodontia. Angle Orthod. 1931;1(1):45-66.
2. Trpkova B, Major P, Prasad N, Nebbe B. Cephalometric landmarks identification and reproducibility: a metaanalysis. Am J Orthod Dentofacial Orthop. 1997 Aug;112(2):165-70.
3. Magalhaes AE, Stella JP, Epker BN. Facial anthropometrics versus cephalometry as predictors for surgical treatment in patients with class III dentofacial deformities. Int J Adult Orthodon Orthognath Surg. 1995;10(4):295-302.
4. Ahmad M, Jenny J, Downie M. Application of cone beam computer tomography in oral and maxillofacial surgery. Aust Dent J. 2012 Mar;57 Suppl 1:82-94.
5. Silva MA, Wolf U, Heinicke F, Bumann A, Visser H, et al. Cone-beam computed tomography for routine orthodontic treatment planning: a radiation dose evaluation. Am J Orthod Dentofacial Orthop. 2008 May;133(5):640.e1-5.
6. Jung PK, Lee GC, Moon CH. Comparison of cone-beam computed tomography cephalometric measurements using a midsagittal projection and conventional two-dimensional cephalometric measurements. Korean J Orthod. 2015 Nov;45(6):282-288.
7. Hariharan A, Diwakar NR, Jayanthi K, Hema HM, Deepukrishna S, et al. The reliability of cephalometric measurements in oral and maxillofacial imaging: Cone beam computed tomography versus two-dimensional digital cephalograms. Indian J Dent Res. 2016 Jul-Aug;27(40):370-377.
8. Schlicher W, Nielsen I, Huang JC, Maki K, Hatcher DC, et al. Consistency and precision of landmark identification in three-dimensional cone beam computed tomography scans. Eur J Orthod. 2012 Jun;34(3):263–275.
9. Brown AA, Scarfe WC, Scheetz JP, Silveira AM, Farman AG. Linear accuracy of cone beam CT derived 3D images. Angle Orthod. 2009 Jan;79(1):150–157.
10. Periago DR, Scarfe WC, Moshiri M, Scheetz JP, Silveira AM, et al. Linear accuracy and reliability of cone beam CT derived 3-dimensional images constructed using an orthodontic volumetric rendering program. Angle Orthod. 2008 May;78(3):387-395.
11. Stratemann SA, Huang JC, Maki K, Miller AJ, Hatcher DC. Comparison of cone beam computed tomography imaging with physical measures. Dentomaxillofac Radiol. 2008 Feb;37(2):80-93.
12. Lagravère MO, Gordon JM, Guedes IH, Flores-Mir C, Carey JP, et al. Reliability of traditional cephalometric landmarks as seen in three-dimensional analysis in maxillary expansion treatments. Angle Orthod. 2009 Nov;79(6):1047–1056.
13. Lagravère MO, Low C, Flores-Mir C, Chung R, Carey JP, et al. Intraexaminer and interexaminer reliabilities of landmark identification on digitized lateral cephalograms and formatted 3-dimensional cone-beam computerized tomography images. Am J Orthod Dentofacial Orthop. 2010 May; 137(5): 598–604.
14. Zamora N, Llamas JM, Cibrián R, Gandia JL, Paredes V. A study on the reproducibility of cephalometric landmarks when undertaking a three-dimensional (3D) cephalometric analysis. Med Oral Patol Oral Cir Bucal. 2012 Jul;17(4):e678–688.
15. Wylie GA, Fish LC, Epker BN. Cephalometrics: a comparison of five analyses currently used in the diagnosis of dentofacial deformities. Int J Adult Orthodon Orthognath Surg. 1987;2(1):15-36.
16. de Oliveira AE, Cevidanes LH, Phillips C, Motta A, Burke B, et al. Observer reliability of three-dimensional cephalometric landmark identification on cone-beam computerized tomography. Oral Surg Oral Med Oral Pathol Oral Radiol Endod. 2009 Feb;107(2):256–265.
17. Shrout PE, Fleiss JL. Intraclass correlations: Uses in assessing rater reliability. Psychol Bull. 1979 Mar;86(2):420-428.
18. Hochberg Y. A sharper Bonferroni procedure for multiple tests of significance. Biometrika. 1988 Dec;75(4):800–803.
19. Lisboa C, Masterson D, Motta AFJ, Motta AT. Reliability and reproducibility of three-dimensional cephalometric landmarks using CBCT: a systematic review. J Appl Oral Sci. 2015 Mar-Apr;23(2):112–119.
20. Caufield PW. Tracing Technique and Identification of Landmarks. In: Jacobson A and Jacobson R, editors. Radiographic Cephalometry, 2nd edn. Hanover Park (IL): Quintessence Publishing. 2006;48-49.
21. Neiva MB, Soares ÁC, Lisboa Cde O, Vilella Ode V, Motta AT. Evaluation of cephalometric landmark identification on CBCT multiplanar and 3D reconstructions. Angle Orthod. 2015 Jan;85(1):11-17.
22. Frongia G, Piancino MG, Bracco AA, Crincoli V, Debernardi CL, et al. Assessment of the reliability and repeatability of landmarks using 3-D cephalometric software. Cranio. 2012 Oct;30(4):255–263.
23. Hassan B, Nijkamp P, Verheij H, Tairie J, Vink C, et al. Precision of identifying cephalometric landmarks with cone beam computed tomography in vivo. Eur J Orthod. 2013 Feb;35(1):38–44.
24. Katkar RA, Kummet C, Dawson D, Moreno Uribe L, Allareddy V, et al. Comparison of observer reliability of three-dimensional cephalometric landmark identification on subject images from Galileos and i-CAT cone beam CT. Dentomaxillofac Radiol. 2013;42(9):20130059.